# Regulation of angiogenesis by a non-canonical Wnt-Flt1 pathway in myeloid cells

**James A. Stefater III**[1,2], **Ian Lewkowich**[3], **Sujata Rao**[1,2], **Giovanni Mariggi**[4], **April C. Carpenter**[1,2], **Adam R. Burr**[5], **Jieqing Fan**[1,2], **Rieko Ajima**[6], **Jeffery D. Molkentin**[5,7], **Bart O. Williams**[8], **Marsha Wills-Karp**[3], **Jeffrey Pollard**[9], **Terry Yamaguchi**[6], **Napoleone Ferrara**[10], **Holger Gerhardt**[4], and **Richard A. Lang**[1,2,*]

[1]The Visual Systems Group, Divisions of Pediatric Ophthalmology and Developmental Biology, Cincinnati Children's Hospital Medical Center, Cincinnati, OH 45229, USA.

[2]Department of Ophthalmology, University of Cincinnati, Cincinnati, OH 45229, USA.

[3]Division of Immunobiology, Cincinnati Children's Hospital Medical Center, Cincinnati, OH 45229, USA.

[4]Vascular Biology Laboratory, London Research Institute, Cancer Research UK, London, WC2 3PX, UK.

[5]Division of Molecular Cardiovascular Biology, Cincinnati Children's Hospital Medical Center, University of Cincinnati, OH 45229, USA.

[6]Cancer and Developmental Biology Laboratory, National Cancer Institute, Frederick, MD 21701, USA.

[7]Howard Hughes Medical Institute, Cincinnati Children's Hospital Medical Center, University of Cincinnati, OH 45229, USA.

[8]Center for Skeletal Disease Research, Van Andel Research Institute, 333 Bostwick NE, Grand Rapids, MI 49503, USA.

[9]Albert Einstein College of Medicine of Yeshiva University, Jack and Pearl Resnick Campus, 1300 Morris Park Avenue, Bronx, NY 10461, USA.

[10]Genentech Inc., 1 DNA Way, South San Francisco, CA 94080, USA

Correspondence and requests for materials should be addressed to R.A.L. (richard.lang@cchmc.org).. *Corresponding author: Division of Pediatric Ophthalmology, Cincinnati Children's Hospital Medical Center, 3333 Burnet Avenue, Cincinnati, OH 45229, Tel: 513-636-2700 (Office), 513-803-2230 (Assistant), Fax: 513-636-4317. Richard.Lang@cchmc.org.

## Abstract

Myeloid cells are a feature of most tissues. Here we show that during development, retinal myeloid cells (RMCs) produce Wnt ligands to regulate blood vessel branching. In the mouse retina, where angiogenesis occurs postnatally[1], somatic deletion in RMCs of the Wnt ligand transporter *Wntless*[2,3] results in increased angiogenesis in the deeper layers. We also show that mutation of *Wnt5a* and *Wnt11* results in increased angiogenesis and that these ligands elicit RMC responses via a non-canonical Wnt pathway. Using cultured myeloid-like cells and RMC somatic deletion of *Flt1*, we show that an effector of Wnt-dependent suppression of angiogenesis by RMCs is Flt1, a naturally occurring inhibitor of vascular endothelial growth factor (VEGF)[4-6]. These findings indicate that resident myeloid cells can use a non-canonical, Wnt-Flt1 pathway to suppress angiogenic branching.

Myeloid cells have a wide array of biological activities that include immune activation, arteriogenesis[7], and regulation of salt balance and blood pressure[8]. Myeloid cells also regulate vascularity. Tumor associated macrophages influence the growth of blood vessels[9] in part because they are a source of VEGFA[10]. Myeloid cells also promote angiogenic branching[11] and anastamosis[12]. Depending on the context, myeloid cells can be either anti-angiogenic[13] or pro-angiogenic[14]. Here we show that RMCs suppress retinal angiogenesis via a Wnt-Flt1 pathway (Fig S1).

Retinal angiogenesis begins on the day of birth in the mouse with the formation of a superficial vascular plexus (Fig. 1a) that lies within the ganglion cell layer[15]. After formation of this superficial plexus by P7 (post-partum day 7), angiogenic sprouts descend vertically through the retinal layers from P8 to P14 (Fig. 1a). At the outer edge of the inner nuclear layer (INL) the vertical angiogenic sprouts turn and simultaneously branch to form a deep vascular plexus (Fig. 1a). Using antibodies to the vascular endothelial cell (VEC) marker endomucin and to the GFP of the *cfms-eGFP* transgene that marks RMCs, we show that myeloid cells have a unique spatial relationship with angiogenic tip cells. At the point of turning and branching in the outer INL, myeloid cells and angiogenic sprouts are in close contact (Fig. S2a). This was confirmed by labeling with isolectin and F4/80 (Fig. S2b). We then took advantage of high-intensity isolectin labeling of VECS and RMCs and performed a 3D reconstruction with false coloring to illustrate the overall topology of the angiogenic tip cell-RMC interaction (Fig. 1b). This showed close contact between the two cell types throughout turn-and-branch angiogenesis in the deep retinal layer. Furthermore, after turning, angiogenic tip cells extend within the plane of the deep retinal layer and remain RMC-associated (Fig. 1c). In further defining RMCs, we showed that CD204 was unique to RMCs with amoeboid morphology in the superficial retinal layer (Fig. S2c, d). By contrast, deep retinal layer RMCs with extended morphology were CD204-negative (Fig. S2c, e). Both layers of RMCs expressed Iba1[16] but at different levels (Fig. S2c-e). This information allowed us to flow sort distinct populations of superficial (CD11b+, F4/80+, CD204+) and deep layer (CD11b+, F4/80+, CD204-) RMCs (Fig. 1d, e).

Based on prior work showing vascular regulation by myeloid Wnt ligands[17] we hypothesized that RMCs might use Wnt ligands to regulate retinal angiogenesis. First, we examined the expression of Wnt ligands and receptors in superficial and deep RMCs

isolated by flow-sorting. RT-PCR analysis of the deep RMC population revealed expression of Wnt5a, Wnt6 and Wnt11, Fzd7 and Fzd8 as well as the co-receptor Lrp5 (Fig. 1f). With the exception of Wnt5b, which was inconsistent, all other Wnt ligands were not detected in deep RMCs. Superficial RMCs expressed similar Wnts and Fzds (Fig. 1f) but also expressed Wnts 2b, 3 and 3a (data not shown).

The challenge of genetic analysis when RMCs express many Wnt ligands was addressed by the generation of a *loxP*-flanked conditional allele for the essential Wnt ligand transporter Wls/GPR177[2,3]. Both superficial and deep RMCs expressed *Wls* (Fig. 1f). *Wls* was deleted using the myeloid cre driver *cfms-icre*[18] which we confirmed was functional in RMCs (Fig. S3a-c). To analyze retinal vasculature, we imaged superficial and deep retinal vessels at P18 (Fig. 2a). Quantification of vessel branch points showed that *cfms-icre* alone had no effect (Fig. 3b). Furthermore, compared with control $Wls^{+/fl}$ mice, $Wls^{+/fl}$; *cfms-icre* animals had a normal superficial vascular plexus (Fig. 2a, green, Fig. 2c). By contrast, the deep vascular layer (Fig. 2a, red, Fig. 2c) showed an overgrowth. Interestingly, no further enhancement of vascular overgrowth was apparent when the myeloid *Wls* deletion was homozygous as in $Wls^{-/fl}$; *cfms-icre* mice (data not shown). Since myeloid cells are positioned below descending vessels at P10, we assessed vessel branching at the base of these sprouts. $Wls^{+/fl}$; *cfms-icre* mice exhibited reduced simple turning (no branches) and single branching, but significantly more multi-branch events (Fig. 2d). As a weighted mean, the branch index was 2.0 in control and 3.2 in the mutant (p<0.0001).

The higher vascular density of the deep layer in $Wls^{+/fl}$; *cfms-icre* mice could reflect enhanced angiogenesis or defective remodeling. To assess this, we counted deep layer branch points in control ($Wls^{fl/+}$) and experimental ($Wls^{fl/+}$; *cfms-icre*) mice over a time-course from P6 to P18 (Fig. 2e). Between P14 and P18 when remodeling predominates (Fig. 2e, red zone) control and mutant graph slopes were nearly identical. By contrast, between P6 and P14 when vessel growth predominates (Fig. 2e, green zone), the slope of the graph is greater in the mutant. There was no difference between control and mutant animals in the number of vertical sprouts connecting superficial and deep layers (Fig. S3d). Combined, the data in Fig. 2 are consistent with a model in which myeloid Wnt ligands suppress branch formation as angiogenic sprouts make contact with deep layer RMCs (Fig. 1b, c). These data were corroborated by the vascular overgrowth phenotype of *Wnt5a*[19] and *Wnt11*[20] heterozygotes (Figs. S3e, f and S4).

Wnt5a and Wnt11 are most often associated with non-canonical Wnt signaling[21]. We thus investigated the possibility that Wnt-dependent suppression of deep retinal angiogenesis was a non-canonical response. Wnt3a, but not Wnt5a, elicited a canonical response in SuperTopflash (STF) reporter cells (Fig. S5a). Some non-canonical Wnt pathways activate a $Ca^{2+}$ flux[21]. To determine whether myeloid Wnts elicited a $Ca^{2+}$ flux, we added Wnt5a to myeloid-like RAW264.7 cells and measured $Ca^{2+}$-dependent Fura-2 dye emission. Recombinant Wnt5a increased intracellular $Ca^{2+}$ compared to untreated controls (Fig. 3a, S5b, c). Furthermore, to assess the requirement for Wls in Wnt ligand secretion, we exposed RAW264.7 cells to medium from $Wls^{fl/fl}$ MEFs transfected with *Wnt5a* or *Wnt5a* and *cre recombinase* plasmids. RAW264.7 cells had increased $Ca^{2+}$ flux in response to *Wnt5a*-transfected MEF medium relative to *Wnt5a*- and *cre*-transfected medium (Fig. 3b). This

validates the role of Wls in secretion of Wnt5a. Combined, these data show that one myeloid Wnt, Wnt5a, does not stimulate a canonical Wnt response but can elicit a $Ca^{2+}$ flux characteristic of some non-canonical Wnt responses.

In recent work, it has been shown that Wnt5a loss-of-function can rescue the defects associated with deletion of the canonical Wnt pathway co-receptors Lrp5/6[22]. This finding has suggested that Lrp5/6 deletion actually represents a non-canonical pathway gain-of-function and that in deleting the non-canonical ligand Wnt5a, there is a re-balancing of pathway activity. This hypothesis is supported by biochemical analysis showing that Wnt5a can bind Lrp6, but does not elicit the phosphorylation required for canonical signaling[22]. Canonical, non-canonical reciprocal pathway inhibition has also been demonstrated[23]. These findings argue that a deletion of Lrp5/6 can define whether a Wnt signaling pathway is canonical or non-canonical. If canonical, an Lrp5/6 deletion will give the same phenotype as ligand deletion. By contrast, if the signaling pathway is non-canonical, the consequence of Lrp5/6 deletion would be opposite to that of ligand mutation. Thus, to determine whether the RMC response was canonical or non-canonical, we generated a *cfms-icre* somatic mutant of the *Lrp5* coreceptor that is expressed in RMCs (Fig. 1f). Since the result was significantly diminished deep vascular layer density in somatic homozygotes (Fig 3c-f), a response opposite to ligand deletion, this provides *in vivo* evidence that the Wnt response is non-canonical. Even though the superficial vascular layer was slightly deficient in somatic homozygotes (Fig. 3e) this was not the reason reduced density in the deep vascular layer as the descending sprout number was unchanged (Fig. 3f).

The VEGF receptor Flt1 (also known as VEGFR1) can suppress angiogenesis because it has limited signaling capacity, a higher affinity for VEGF than Flk1 (VEGFR2) and can sequester VEGF[5,6]. Alternative splicing produces both membrane tethered (mFlt1) and soluble (sFlt1) forms[5]. Flt1 is known to contribute to corneal avascularity[4] as well as the selection of angiogenic tip cells when expressed regionally in an existing vessel[24]. Flt1 is also known to be expressed in some myeloid populations[6]. Since angiogenesis in the deep retinal layers is VEGF-dependent[25], Flt1 was a good candidate to mediate Wnt-dependent angiogenic suppression by deep RMCs.

We thus determined whether *Flt1* was expressed in P12 RMCs by performing end-point RT-PCR on flow-sorted cells using primers that detected both transcripts. This showed that deep RMCs expressed *Flt1* (Fig. 4a). By contrast, superficial RMCs did not (Fig. 4a). We also showed that Iba1-labeled RMCs positioned at the outer edge of the INL labelled with anti Flt1 antibodies (Fig. 4b). We then generated an RMC *Flt1* loss-of-function using *cfms-icre* and the *Flt1^fl* conditional allele[26]. Quantification of retinal vascular branch points in *Flt1^{+/fl}*; *cfms-icre* mice at P18 showed that the superficial layer was unaffected but that the deep layer showed an increase in density (Fig. 4c, d). As with *Wls* somatic mutants, conditional homozygosity for *Flt1* (*Flt1^{fl/fl}*; *cfms-icre*) did not give a further significant increase in vascular density (data not shown). Furthermore, the number of deep RMCs was unchanged (Fig. S2g).

These data showed that conditional deletion of *Flt1* produced an enhancement of angiogenesis similar to that observed with conditional deletion of *Wls*. One implication was

that Wls and Flt1 might function in the same angiogenesis suppression pathway. To test the possibility that *Flt1* might be regulated by Wnt ligands, we used myeloid-like RAW264.7 cells that, like RMCs, express *Fzd7* and *Fzd8* (Fig. 4e). When stimulated with the "canonical" ligand Wnt3a, RAW264.7 did not change the level of *Flt1* transcript according to QPCR (Fig. 4f). However, stimulation with Wnt5a produced a 3-fold increase in the level of both Flt1 isoform transcripts (Fig. 4f). Furthermore, an ELISA showed that there was an increased level of sFlt1 in conditioned media from Wnt5a stimulated RAW264.7 cells (Fig. 4g). Wnt3a stimulation again had no effect (Fig. 4g).

As a stringent test of the possibility that Wnt ligands stimulated expression of *Flt1* in deep RMCs, we flow sorted the CD11b+, F4/80+, CD204-population from both control (*Wls$^{+/fl}$*) and experimental (*Wls$^{+/fl}$; cfms-icre*) mice at P12 and performed QPCR for *Flt1* transcripts. We were never able to amplify the mFlt1 transcript but showed that there was a 90% reduction in transcript level for sFlt1 (Fig. 4h). This was consistent with the maximal phenotype observed in the heterozygous conditional *Wls* mutants. Though a heterozygous phenotype is not unusual, it is perhaps surprising that conditional homozygosity gave no further significant change. This kind of response might be explained by a low signaling sensitivity threshold for the Wnt-Flt1 pathway.

The data we describe reveal that RMCs can directly modulate angiogenic responses by producing the VEGF inhibitory receptor Flt1. Unexpectedly, we also show that the production of Flt1 depends on myeloid non-canonical Wnt ligands. In this setting, myeloid Wnt ligands might function in autocrine stimulation as has been documented for cultured macrophages[27] or might operate via a more complex pathway involving another cell type as an intermediate. The Wnt-Flt1 response represents a new pathway for the regulation of VEGF-stimulated angiogenesis. The targeting of appropriate Fzd receptors or other Wnt-Flt1 pathway components may offer new opportunities to modulate the production of Flt1 and thus, the VEGF-stimulated angiogenic response. Since macrophage-related cells are ubiquitous and highly mobile, it is possible that the Wnt-Flt1 pathway will be a general means to suppress VEGF locally and thus to tamp-down vascular responses. In future studies it will be interesting to determine, for example, if this pathway is active in the suppression of wound angiogenesis by macrophages[13] or is inactivated in macrophage-dependent tumor angiogenesis[28].

Additionally, our observations are consistent with a string of recent papers expanding the role of myeloid cells beyond their well-documented functions in innate immunity[7,8,17,29]. These findings build on an idea articulated by Ilya Metchnikoff nearly a century ago. He suggested that phagocytes originally evolved to regulate developmental processes, and that their immune functions were a later evolutionary adaptation. He proposed that macrophages were the "policemen" of multi-cellular organisms, and that they, in his words, could establish "harmony from chaos."[30] Here we show, in the setting of the retina, that myeloid cells do just that by fine-tuning vascular density and directing vascular traffic.

## Methods Summary

We prepared and stained retinas as previously reported[1]. To isolate RMCs, we digested retinas, pre-enriched with CD11b beads, and sorted for surface makers with the FACSAria II. To obtain conditioned medium from MEFs, we performed transient transfections with Wnt5a, Thy1.1 and cre plasmids, sorted Thy1.1-positive MEFS, and re-plated transfected cells. We performed calcium imaging on RAW264.7 cells loaded in Ringer's solution with 5 μM Fura-2 AM and imaged at 510 nm at 1 Hz after excitation at 340 nm and 380 nm. All animal experiments were performed in accordance with IACUC-approved guidelines and regulations.

## Methods

### Quantification of retinal vasculature and isolation of RMCs

Retinas were prepared and imaged as reported[1] except that Alexa Fluor 488 isolectin GS-IB$_4$ (Invitrogen) was used to label retinal vessels and RMCs. Other Abs included anti-endomucin (Santa Cruz, V.7C7), anti-GFP (Abcam), anti-Iba1 (Wako), anti-CD204 (AbD Serotec), and anti-Flt1 (R&D). For quantification, we used 200× magnification images located at the retinal periphery between artery and vein. For each genotype, at least 3 fields were analyzed from at least 4 animals from a minimum of 2 litters. Control and experimental animals were littermates. This minimized the effect of strain background in producing variation in vascular density[31-34]. For flow sorting, retinas were digested and sorted as reported[16] except that 0.5 mg/mL DNase II (Sigma Aldrich) was used. Furthermore, myeloid cells were pre-enriched using CD11b beads (Miltenyi Biotech). Cells were then incubated with anti-CD16/32 (clone 24.G2) for 30 minutes and labelled with mAbs to PE-Cy7 conjugated anti-CD11b (clone M1/70), APC-Cy7 or PerCP-Cy5.5 conjugated anti-F4/80 (clone BM8), Alexa-647 conjugated anti-CD204 (clone 2F8), and 7-AAD. Cells were sorted with FACSAria II running DiVa software.

### RNA Isolation and RT-PCR

RNA was isolated using RNeasy (Qiagen). QPCR was performed with QuantiTect SYBR green (Qiagen). Primers are listed in Supplementary Table 1.

### *In Vitro* Analysis

MEFs were isolated as described[35] from *Wls*$^{flfl}$ mice[36] and transfected with combinations of 2.5 μg Wnt5a, Thy1.1 and cre plasmids using TransIT-2020 (Mirus). MEFs were sorted using magnetic beads for Thy1.1, replated and supernatant was collected after 24 hours. RAW264.7 cells (ATCC) were cultured in DMEM (10% FBS) and treated with recombinant Wnt3a (10 ng/mL, R&D) or Wnt5a (500 ng/mL, R&D). ELISA was performed using the sVEGFR1 Quantikine kit (R&D). For calcium imaging, RAW264.7 cells were loaded in Riger's solution with 5 μM Fura-2 AM and imaged at 510 nm at 1 Hz after excitation at 340 nm and 380 nm. Data was acquired using EasyRatioPro. Ca$^{2+}$ traces are 50-cell averages from 2 experiments.

## Statistics

All statistical tests used are stated in the figure legends. In analyzing QPCR data, the p values refer to a comparison of the     cT values.

## Animals

Breeding and genotyping of $Wls^{fl}$ (ref [36]), *cfms-icre* (ref 18), Z/EG (ref 37), $Wnt5a^{+/-}$ (ref 19), $Wnt11^{+/-}$ (ref 20) and $Flt^{fl}$ (ref 26) was performed as previously described. $Lrp5^{fl}$ will be described in detail in a forthcoming publication. The allele is a conventional design where exon 2 of the Lrp5 gene is flanked by LoxP sites. It has been confirmed that deletion between the LoxP sites produces a loss-of-function. All animal experimentation was carried out using protocols approved by the Institutional Animal Care and Use Committee.

# Supplementary Material

Refer to Web version on PubMed Central for supplementary material.

# Acknowledgements

# References

1. Gerhardt H, et al. VEGF guides angiogenic sprouting utilizing endothelial tip cell filopodia. J Cell Biol. 2003; 161:1163–1177. [PubMed: 12810700]

2. Ching W, Nusse R. A dedicated Wnt secretion factor. Cell. 2006; 125:432–433. [PubMed: 16678089]

3. Carpenter AC, Rao S, Wells JM, Campbell K, Lang RA. Generation of mice with a conditional null alelle for *Wntless*. Genesis. 2010; 48:554–558. [PubMed: 20614471]

4. Ambati BK, et al. Corneal avascularity is due to soluble VEGF receptor-1. Nature. 2006; 443:993–997. [PubMed: 17051153]

5. Kendall RL, Thomas KA. Inhibition of vascular endothelial cell growth factor activity by an endogenously encoded soluble receptor. Proc Natl Acad Sci U S A. 1993; 90:10705–10709. [PubMed: 8248162]

6. Shibuya M. Structure and dual function of vascular endothelial growth factor receptor-1 (Flt-1). Int J Biochem Cell Biol. 2001; 33:409–420. [PubMed: 11312109]

7. Pipp F, et al. VEGFR-1-selective VEGF homologue PlGF is arteriogenic: evidence for a monocyte-mediated mechanism. Circ Res. 2003; 92:378–385. [PubMed: 12600898]

8. Machnik A, et al. Macrophages regulate salt-dependent volume and blood pressure by a vascular endothelial growth factor-C-dependent buffering mechanism. Nat Med. 2009; 15:545–552. [PubMed: 19412173]

9. Lin EY, Pollard JW. Tumor-associated macrophages press the angiogenic switch in breast cancer. Cancer Res. 2007; 67:5064–5066. [PubMed: 17545580]

10. Stockmann C, et al. Deletion of vascular endothelial growth factor in myeloid cells accelerates tumorigenesis. Nature. 2008

11. Kubota Y, et al. M-CSF inhibition selectively targets pathological angiogenesis and lymphangiogenesis. J Exp Med. 2009; 206:1089–1102. [PubMed: 19398755]

12. Fantin A, et al. Tissue macrophages act as cellular chaperones for vascular anastomosis downstream of VEGF-mediated endothelial tip cell induction. Blood. 2010; 116:829–840. [PubMed: 20404134]

13. Martin P, et al. Wound healing in the PU.1 null mouse--tissue repair is not dependent on inflammatory cells. Curr Biol. 2003; 13:1122–1128. [PubMed: 12842011]

14. Grunewald M, et al. VEGF-induced adult neovascularization: recruitment, retention, and role of accessory cells. Cell. 2006; 124:175–189. [PubMed: 16413490]

15. Saint-Geniez M, D'Amore PA. Development and pathology of the hyaloid, choroidal and retinal vasculature. Int J Dev Biol. 2004; 48:1045–1058. [PubMed: 15558494]

16. Mendes-Jorge L, et al. Scavenger function of resident autofluorescent perivascular macrophages and their contribution to the maintenance of the blood-retinal barrier. Invest Ophthalmol Vis Sci. 2009; 50:5997–6005. [PubMed: 19608545]

17. Lobov IB, et al. WNT7b mediates macrophage-induced programmed cell death in patterning of the vasculature. Nature. 2005; 437:417–421. [PubMed: 16163358]

18. Deng L, et al. A novel mouse model of inflammatory bowel disease links mammalian target of rapamycin-dependent hyperproliferation of colonic epithelium to inflammation-associated tumorigenesis. Am J Pathol. 2010; 176:952–967. [PubMed: 20042677]

19. Yamaguchi TP, Bradley A, McMahon AP, Jones S. A Wnt5a pathway underlies outgrowth of multiple structures in the vertebrate embryo. Development. 1999; 126:1211–1223. [PubMed: 10021340]

20. Majumdar A, Vainio S, Kispert A, McMahon J, McMahon AP. Wnt11 and Ret/Gdnf pathways cooperate in regulating ureteric branching during metanephric kidney development. Development. 2003; 130:3175–3185. [PubMed: 12783789]

21. Seifert JR, Mlodzik M. Frizzled/PCP signalling: a conserved mechanism regulating cell polarity and directed motility. Nat Rev Genet. 2007; 8:126–138. [PubMed: 17230199]

22. Bryja V, et al. The extracellular domain of Lrp5/6 inhibits noncanonical Wnt signaling in vivo. Mol Biol Cell. 2009; 20:924–936. [PubMed: 19056682]

23. Grumolato L, et al. Canonical and noncanonical Wnts use a common mechanism to activate completely unrelated coreceptors. Genes Dev. 24:2517–2530. [PubMed: 21078818]

24. Chappell JC, Taylor SM, Ferrara N, Bautch VL. Local guidance of emerging vessel sprouts requires soluble Flt-1. Dev Cell. 2009; 17:377–386. [PubMed: 19758562]

25. Haigh JJ, et al. Cortical and retinal defects caused by dosage-dependent reductions in VEGF-A paracrine signaling. Dev Biol. 2003; 262:225–241. [PubMed: 14550787]

26. Lichtenberger BM, et al. Autocrine VEGF signaling synergizes with EGFR in tumor cells to promote epithelial cancer development. Cell. 2010; 140:268–279. [PubMed: 20141840]

27. Blumenthal A, et al. The Wingless homolog WNT5A and its receptor Frizzled-5 regulate inflammatory responses of human mononuclear cells induced by microbial stimulation. Blood. 2006; 108:965–973. [PubMed: 16601243]

28. Stockmann C, et al. Deletion of vascular endothelial growth factor in myeloid cells accelerates tumorigenesis. Nature. 2008; 456:814–818. [PubMed: 18997773]

29. Lin SL, et al. Macrophage Wnt7b is critical for kidney repair and regeneration. Proc Natl Acad Sci U S A. 2010; 107:4194–4199. [PubMed: 20160075]

30. Tauber AI. Metchnikoff and the phagocytosis theory. Nat Rev Mol Cell Biol. 2003; 4:897–901. [PubMed: 14625539]

31. Rohan RM, Fernandez A, Udagawa T, Yuan J, D'Amato RJ. Genetic heterogeneity of angiogenesis in mice. Faseb J. 2000; 14:871–876. [PubMed: 10783140]

32. Gao G, et al. Difference in ischemic regulation of vascular endothelial growth factor and pigment epithelium--derived factor in brown norway and sprague dawley rats contributing to different susceptibilities to retinal neovascularization. Diabetes. 2002; 51:1218–1225. [PubMed: 11916948]

33. Chan CK, et al. Mouse strain-dependent heterogeneity of resting limbal vasculature. Invest Ophthalmol Vis Sci. 2004; 45:441–447. [PubMed: 14744883]

34. Chan CK, et al. Differential expression of pro- and antiangiogenic factors in mouse strain-dependent hypoxia-induced retinal neovascularization. Lab Invest. 2005; 85:721–733. [PubMed: 15856049]

35. Nagy, A.; Gertsenstein, M.; Vintersten, K.; Behringer, RR.; M, G. Manipulating the mouse embryo: a laboratory manual. 3 edn. Cold Spring Harbor Laboratory Press; 2002. p. 371-373.

36. Carpenter AC, Rao S, Wells JM, Campbell K, Lang RA. Generation of mice with a conditional null allele for Wntless. Genesis. 2010; 48:554–558. [PubMed: 20614471]

37. Novak A, Guo C, Yang W, Nagy A, Lobe CG. Z/EG, a double reporter mouse line that expresses enhanced green fluorescent protein upon Cre-mediated excision. Genesis. 2000; 28:147–155. [PubMed: 11105057]
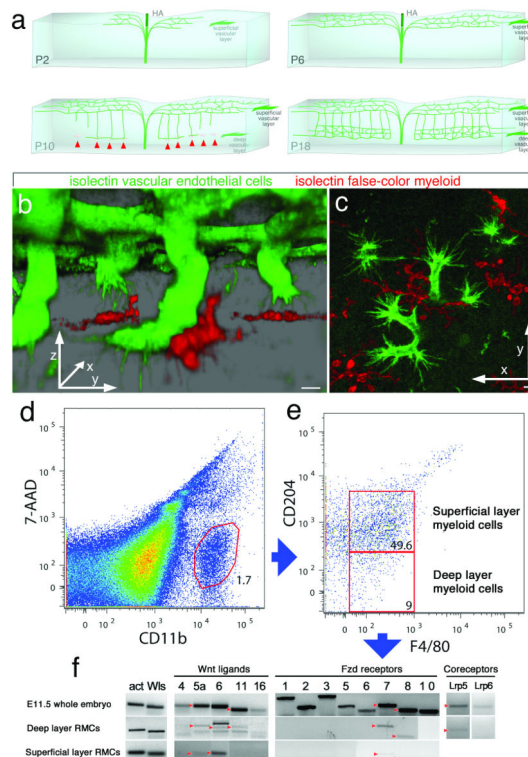
**Figure 1. RMCs interact with VECs and express Wnt components**

(a) Schematic of retina at postnatal days (P) 2, 6, 10, and 18. RMCs interacting with descending vertical sprouts are labeled with red arrowheads. Adapted from Ref 1. (b) Isolectin-labeled 3D reconstruction of vertical angiogenic sprouts (green) and RMCs (false-color red). (c) As in (b) but a 2D image in the deep vascular layer. 5 μm scale bars. (d, e) Flow-sorting of deep layer RMCs based on surface markers. (f) PCR for Wnt pathway components on flow-sorted RMCs. Red arrowheads indicate expected sizes.
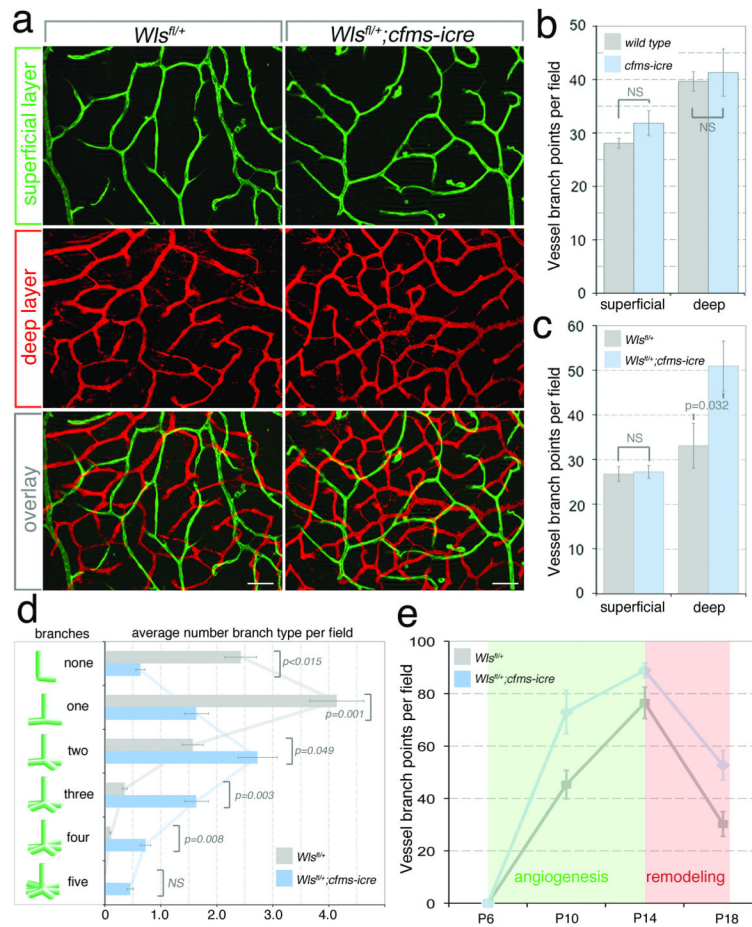
**Figure 2. RMC *Wls* is required for suppression of deep angiogenic branching**
(a) Isolectin labeling of superficial and deep retinal vasculature in $Wls^{+/fl}$ and $Wls^{+/fl}$; *cfms-icre* mice. 50 µm scale bars. (b, c) P18 vessel branch points in labeled genotypes. n=4 (b), n=8 (c). (d) Branches emanating from the base of vertical sprouts in the P10 deep vascular layer. n=8. (b-d) Used Student's T-test (two-tailed). (e) Time-course of deep layer branches in indicated genotypes. Shading shows when angiogenesis (green) and remodeling (red) predominate. One Way ANOVA revealed p=0.0021. n=4 for each point. Errors are SEM. NS – Not significant.
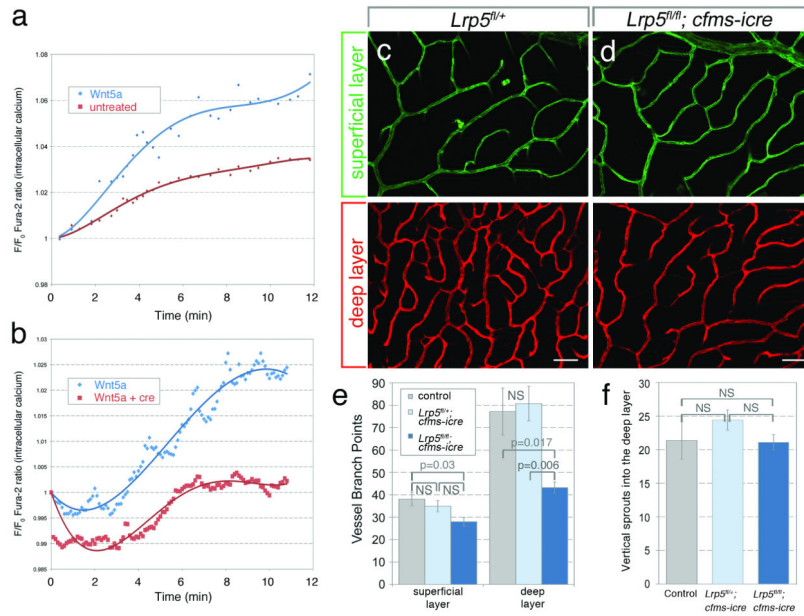
**Figure 3. Angiogenic suppression by RMCs is a non-canonical Wnt response**

(a, b) Intracellular $Ca^{2+}$ in RAW264.7 cells treated with Wnt5a (a) or supernatant from *Wls^{fl/fl}* MEFs expressing *Wnt5a* or *Wnt5a* and *cre* (b). One Way ANOVA showed $p<0.0001$ for both. (c, d) Isolectin labeling of superficial and deep retinal vasculature in *Lrp5^{+/fl}* (c) and *Lrp^{fl/fl}; cfms-icre* (d) mice. 50 µm scale bars. (e) P18 vessel branch points in labeled genotypes. (f) Vertical vessels connecting to the deep layer in labeled genotypes. (e, f) Used One Way ANOVA with Tukey's post-hoc. n 8 per genotype. Errors are SEM. NS – not significant.
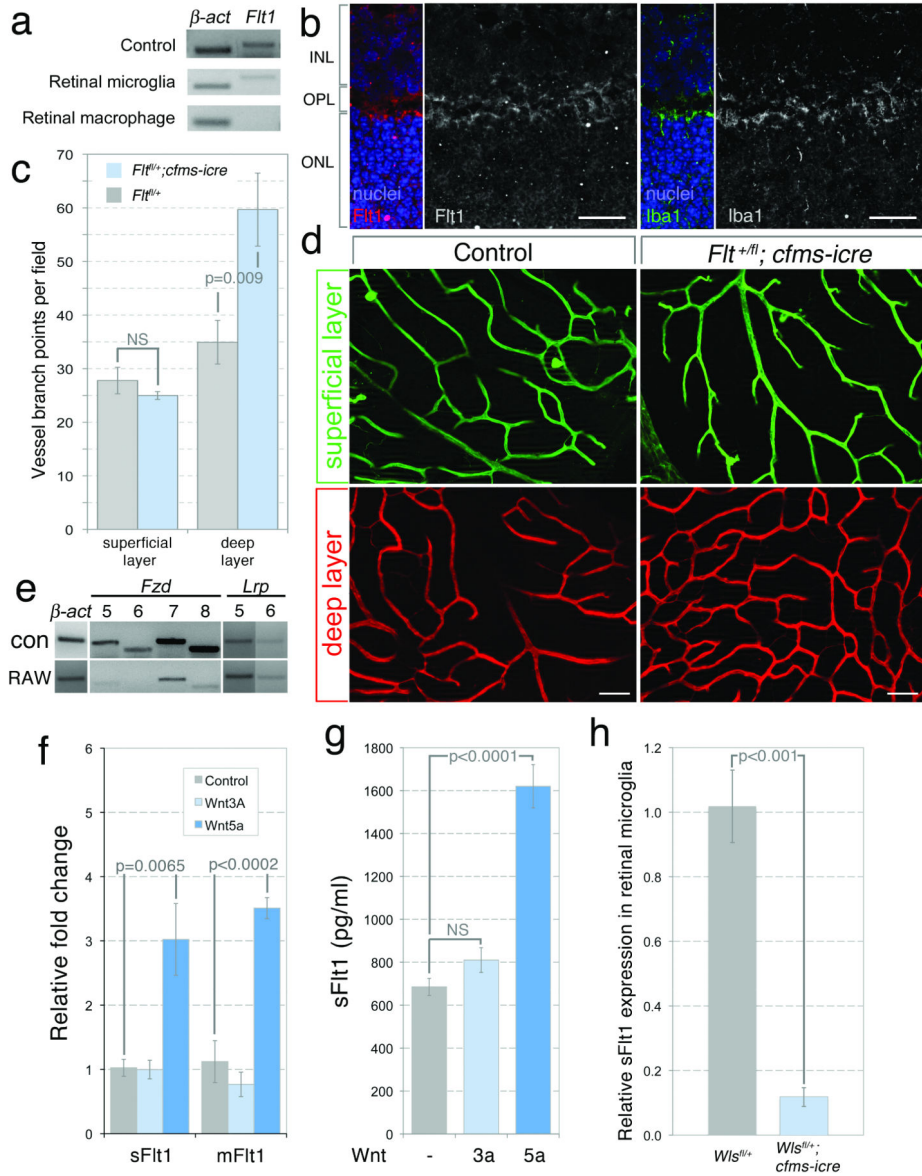
**Figure 4. Flt1 expression in myeloid cells is regulated by a Wnt pathway**

(a) PCR for Flt1 transcript in flow-sorted RMCs. (b) P14 retinal sections labeled for Flt1 and Iba1. 25 μm scale bars. (c) P18 vessel branch points in the superficial and deep vasculature in *Flt1+/fl* and *Flt1+/fl; cfms-icre* mice (n=7, Student's T-test). n=7. (d) Isolectin labeling of the retinal vasculature in labeled genotypes. 50 μm scale bars. (e) PCR for indicated transcripts in E11.5 whole embryo (con) and RAW264.7 cells. (f, g) QPCR (f) for sFlt1 and mFlt1 in Wnt-treated RAW264.7 cells and ELISA (g) for sFlt1 on medium from Wnt-treated RAW264.7 cells (n=4, One Way ANOVA). (h) QPCR for sFlt1 in flow-sorted deep RMCs from *Wls+/fl* and *Wls+/fl; cfms-icre* mice (n=4, Student's T-test). Errors are SEM. NS – Not significant.